ISSN 0036-0236, Russian Journal of Inorganic Chemistry, 2016, Vol. 61, No. 11, pp. 1387–1391. © Pleiades Publishing, Ltd., 2016.
Original Russian Text © A.S. Lyadov, A.A. Kochubeev, L.D. Koleva, O.P. Parenago, S.N. Khadzhiev, 2016, published in Zhurnal Neorganicheskoi Khimii, 2016, Vol. 61, No. 11, pp. 1440–1444.

SYNTHESIS AND PROPERTIES OF INORGANIC COMPOUNDS

Synthesis of Nanosized Iron(III) Oxide and Study of Its Formation Features

A. S. Lyadov*, A. A. Kochubeev, L. D. Koleva, O. P. Parenago, and S. N. Khadzhiev
Topchiev Institute of Petrochemical Synthesis, Russian Academy of Sciences, Leninskii pr. 29, Moscow, 119991 Russia
**e-mail: lyadov@ips.ac.ru*

Received January 28, 2016

Abstract—Nanosized iron(III) oxide has been obtained by thermolysis of iron(III) acetylacetonate using diphenyl ether as a dispersion medium. It has been shown that increase in thermolysis temperature from 180 to 250°C allows one to half the average size of Fe_2O_3 nanoparticles. The introduction of surfactant into dispersion medium also leads to decrease of the average size of particles down to 4 nm. The phase composition of the prepared nano-Fe_2O_3 has been established, the possibility to reduce nano-Fe_2O_3 into iron metal has been shown by temperature-programmed reduction

DOI: 10.1134/S0036023616110127

At present, nanosized iron(III) oxide and composite materials on its basis find a wide application in various fields of science and technology. For example, nanosized iron(III) oxide can be used in catalysis as a catalyst in Fisher–Tropsch process [1], cyclocondensation reaction, and photocatalysis [2]. This compound is used in medicine as a contrast substance in MRT diagnostics [3] or for precise delivery of pharmaceuticals [4], it is applied in power technology as electrodes in alkaline batteries [5], etc. Nanosized iron oxide is also applied in the manufacture of dyes, sorbents, and gas sensors. Superparamagnetism is another useful property of nanosized iron oxide [6].

There is the large number of methods for preparing nanosized iron oxide, thermolysis of iron-containing precursors under specially selected dispersion media plays an important role among them. It should be noted that variation of precursor nature, dispersion medium, and thermolysis conditions provides a possibility to change considerably the morphology and size of resulting iron oxide particles. The introduction of surfactants into dispersion medium in the course of thermolysis process is an important feature because these compounds provide not only stabilization of nanoparticles but also change of their size and morphology. Dispersion media commonly used are high-boiling thermally stable liquids, for example, paraffin hydrocarbons [7], ethers [8], and polyhydric alcohols [9]. Thus, glycerol found a wide application in the synthesis of various nanoparticles, while the method itself is called glycothermal synthesis [10].

Inorganic salts (halides, nitrate, sulfate, carbonyls, etc.) and iron complexes are used as precursors for the preparation of iron oxide nanoparticles. In recent time, acetylacetonates of *d*-block elements are often used as precursors to prepare the corresponding nanoparticles. These compounds are chosen because they are cheap, simple to prepare, show low toxicity, low decomposition temperature, and their thermolysis results in formation of particles of the same shape with monodisperse distribution [11].

The aim of this work is to study the features of formation of nanosized iron(III) oxide in the course of thermolysis of iron(III) acetylacetonate $Fe(acac)_3$ in diphenyl ether medium under varying synthesis conditions and to study physicochemical properties of prepared nano-Fe_2O_3.

EXPERIMENTAL

We used $Fe(acac)_3$ as a precursor of nanosized iron-containing particles, the compound is well soluble in organic solvents and contains no water, which is favorable for the course of thermolysis and formation of nanosized particles. Iron(III) acetylacetonate was synthesized by procedure [12] and identified by X-ray powder diffraction and UV spectroscopy. The synthesis of nanoparticles was carried out by thermolysis of the precursor in diphenyl ether (DPE), which is an aromatic ether insoluble in water but well soluble in organic solvents; it has boiling point 259°C, which considerably increases with pressure. This compound was selected as a dispersion medium because of rather high boiling point and low toxicity.

To prepare nanosized iron(III) oxide, 0.5 g of $Fe(acac)_3$ was dissolved in 10 mL of DPE or a mixture of DPE with the appropriate amount of surfactant. Next, 40 mL of DPE or a DPE–surfactant mixture

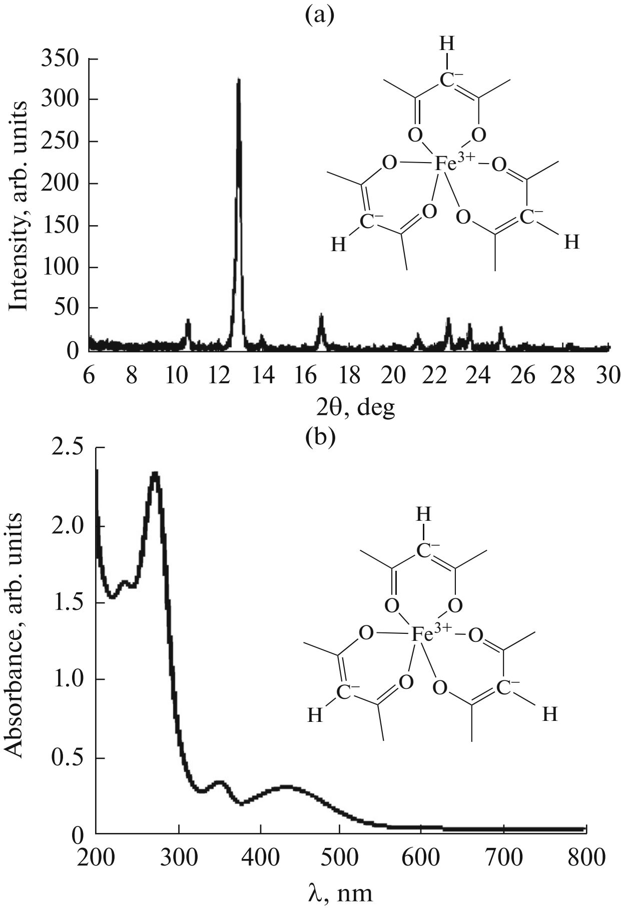

Fig. 1. X-ray diffraction pattern of $Fe(acac)_3$ (a) and UV spectrum of $Fe(acac)_3$ in ethanol (b).

was heated to required temperature on an oil bath with vigorous magnetic stirring in a two-necked round-bottomed flask equipped with a reflux condenser. Next, a solution of $Fe(acac)_3$ was quickly added via a syringe into the hot DPE or DPE–surfactant solution. The resultant mixture was kept for 2 h with vigorous stirring for complete thermolysis and formation of nanosized particles. Then, the mixture was cooled and analyzed.

The thermal analysis of the precursor was conducted on a Q-600 thermal analyzer in temperature range 25–1000°C in air at heating rate 10 K/min.

Absorption spectra in the visible and ultra-violet region were recorded on a Shimadzu UV-2401PC spectrometer in the range 200–800 nm in quartz cuvettes transparent in the UV region. Optical path length of cuvette was 1 mm.

Iron(III) acetylacetonate and prepared samples were studied by X-ray powder diffraction analysis (XRD) on a Rigaku X-ray diffractometer with an Ultima IV θ–θ goniometer using CoK_α radiation with scanning step of 0.02° and counting time 1 s. The range of measurement angles $2\theta = 10°–100°$.

The indexing of X-ray diffraction patterns of the prepared compounds was conducted by homology method on the basis of data taken from the ICDD PDF-4 international database.

Particle size and sample morphology was determined by transmission electron microscopy (TEM) on a Tecnai Spirit 120 kV electron microscope. Analyzed specimen was dispersed in methanol using ultrasound and then applied on a copper support.

The features of reduction of nanosized iron(III) oxide were studied by temperature-programmed reduction (TPR) on a Micromeritics Auto Chem II instrument. For this purpose, a specimen was placed into a quartz U-shaped reactor equipped with a thermocouple and heated in a gas mixture (5 vol % of hydrogen in argon) to 900°C. Gas mixture supply rate was 50 mL/min, heating rate 0.167 K/s, temperature inside the reactor being measured (the thermocouple was disposed at 5 mm from specimen surface) and reducing agent consumption was measured with a thermal conductivity detector (TCD).

RESULTS AND DISCUSSION

Prepared $Fe(acac)_3$ was analyzed by XRD analysis and UV spectroscopy to identify the obtained compound. Figures 1a and 1b show the obtained results. The diffractogram (Fig. 1a) shows the presence of distinct peaks, which indicates that obtained $Fe(acac)_3$ has well formed monophasic crystal structure. On the basis of comparison of the obtained diffraction pattern with data taken from ICDD PDF-4 database, one can draw a conclusion that the prepared $Fe(acac)_3$ is isostructural to the complexes described in the literature. The UV spectrum of iron(III) acetylacetonate solution in ethanol (Fig. 1b) exhibits four peaks in the wavelength region 200–800 nm [13]. The first (≈436 nm) and second (≈350 nm) weak peaks in the visible and near UV spectral regions are caused by *d*–*d* transitions (the transitions of central ion electrons between split energetic levels, difference between them is determined by the strength and symmetry of the given ligand field). The weak intensity of these peaks is caused by the fact that these transitions are forbidden by selection rules. The presence of chromophore groups in acetylacetonate ligands (C=C, C=O) provides the emergence in spectrum of peaks typical for $n\pi^*$ (the third peak at ≈275 nm) and $\pi\pi^*$ (the fourth peak at ≈230 nm) transitions.

Since the synthesis of iron oxide nanoparticles was performed by thermolysis of iron acetylacetonate, it was of interest to carry out its thermal analysis. Figure 2 shows the obtained thermogram. The decomposition of $Fe(acac)_3$ begins at 169°C, while the most active weight loss is observed in the range 169–295°C and results in 60% weight loss. The decomposition of iron acetylacetonate is characterized by a set of exo effects.

Figure 3 displays the micrographs of nanosized iron oxide particles obtained in the absence of surfac-

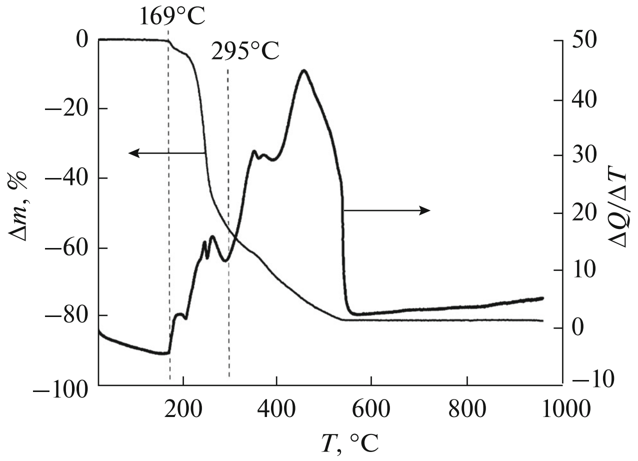

Fig. 2. Thermogram of iron(III) acetylacetonate.

tant. It is seen that at low-temperature thermolysis (180°C, Fig. 3a) the particles differ in form, there is a trend to form particles of triangle shape, the average size is 12–15 nm. Increase in thermolysis temperature leads not only to decrease of average particle size but also formation of particles of uniform shape (Fig. 3b). Increase in thermolysis temperature from 180 to 250°C provides more than twofold decrease of average size of iron(III) oxide particles (Fig. 3c).

The introduction of surfactants is known to allow the preparation of particles of smaller size, other synthesis conditions being equal. In this work, we used a mixture of oleic acid, oleylamine, and oleyl alcohol in 1 : 1 : 1 weight ratio as a surfactant. The introduction of 5 wt % of the surfactant into dispersion medium leads to formation of uniform in shape nanosized particles even at thermolysis temperature of 180°C (Fig. 4a), increase in surfactant concentration allows one to decrease considerably the size of particles (Fig. 4b). Thus, at surfactant concentration of 15 wt % and thermolysis temperature of 180°C, the average size of iron oxide particles is only 4 nm.

To study the physicochemical properties of nanosized iron(III) oxide, we used a sample obtained by the thermolysis of Fe(acac)$_3$ in DPE in the absence of surfactant at 200°C. The average size of particles of such a sample was 8–9 nm. To study the phase composition of nano-Fe$_2$O$_3$ and its ability to reduction, we obtained solid iron(III) oxide nanoparticles as a black powder by the removal of DPE in a vacuum.

Figure 5a shows X-ray diffraction pattern for nanosized iron(III) oxide with average particle size of 8–9 nm, which is characterized by the presence of well-formed slightly broadened peaks indicating a small size of crystallites. The nanosized Fe$_2$O$_3$ has a cubic structure (PDF #39-1346). The use of the Scherrer equation [14] allowed us to calculate the average size of crystallites for this sample:

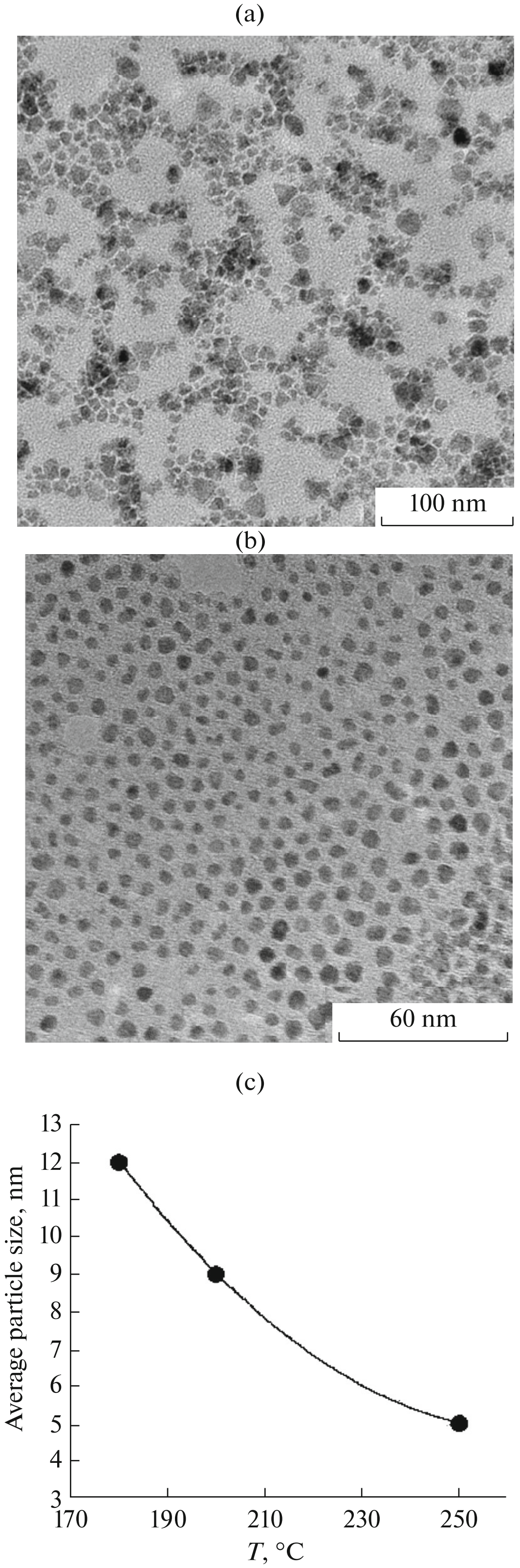

Fig. 3. TEM image of nano-Fe$_2$O$_3$: (a) thermolysis at 180°C, (b) thermolysis at 250°C, dependence of particle size on thermolysis temperature (c).

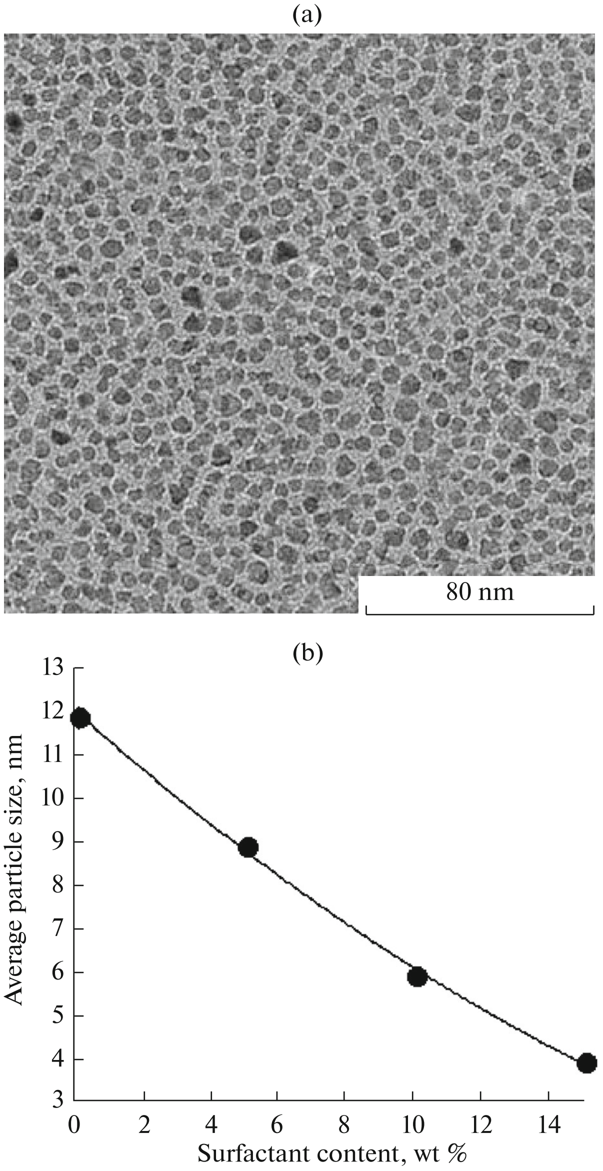

Fig. 4. TEM image of nanosized iron(III) oxide prepared in the presence of surfactant by thermolysis at 180°C (a), effect of surfactant concentration on the average size of resulting nano-Fe_2O_3 particles (b).

$$L = \frac{0.94\lambda}{B(2\theta)\cos(\theta)} = \frac{0.94 \times 0.178897}{0.019\cos(20.51)} = 9 \text{ nm}.$$

The obtained from XRD data crystallite size (9 nm) agrees well with the results of TEM for the sample under study.

The TPR profile of nanosized iron oxide (Fig. 5b) has three peaks of hydrogen absorption, which corresponds to three consecutive reduction processes. The following processes are most likely to take place in the course of reduction [15]:

$$\text{I peak: } Fe_2O_3 \rightarrow Fe_3O_4,$$

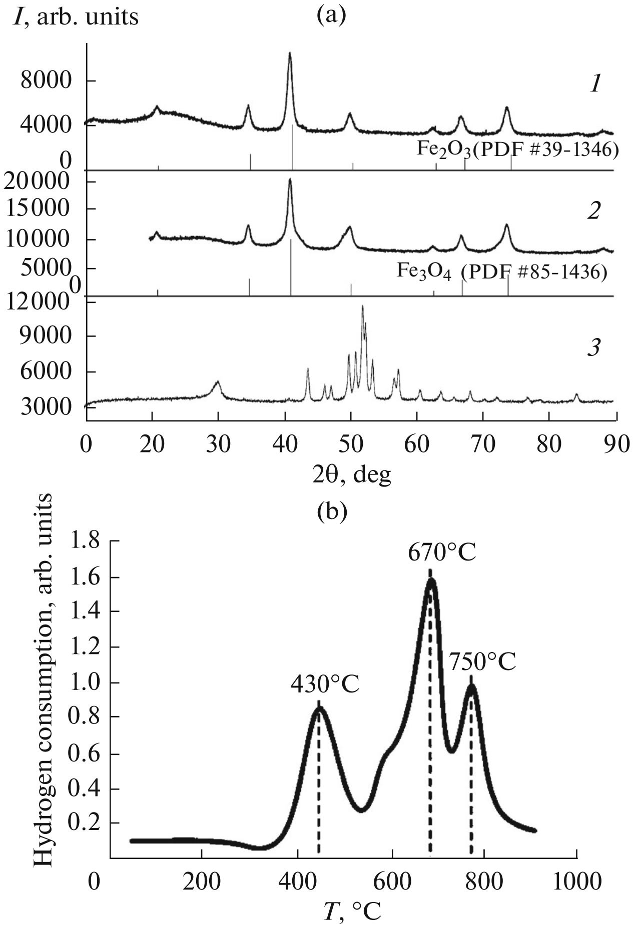

Fig. 5. X-ray diffraction patterns (a): (*1*) nano-Fe_2O_3; (*2*) the sample after reduction at 430°C; (*3*) the sample after reduction at 670°C; TPR profile of nano-Fe_2O_3 (b).

$$\text{II peak: } Fe_3O_4 \rightarrow Fe_{1-x}O,$$

$$\text{III peak: } Fe_{1-x}O \rightarrow Fe.$$

To confirm this scheme, we determined the phase composition of reduction products. The X-ray diffraction patterns of these samples are shown in Fig. 5a. In the reduction of nano-Fe_2O_3 at 430°C until completion of hydrogen absorption, a phase of magnetite really forms, which has a cubic structure like initial nano-Fe_2O_3 (PDF #85-1436). The crystallographic difference in the cubic structure of Fe_2O_3 and Fe_3O_4 is not larger 1%, therefore the X-ray diffraction patterns of these compounds are very similar and their identification by this method is often difficult. Further increase in magnetite reduction temperature up to 670°C leads to formation of multiphase product (Fig. 5a, *3*). The X-ray diffraction pattern shows numerous reflections, including reflections related to iron monooxide (wüstite), iron metal, and different carbide forms of iron. The formation of carbides is possible because of incomplete removal of diphenyl ether during vacuum distillation. Diphenyl ether residue undergoes decomposition on the surface of nanoparticles to produce carbon, which reacts at high temperature with iron-containing compounds to give carbide phases. Iron metal is the final product of complete reduction of nano-Fe_2O_3.

Thus, we performed the synthesis of nanosized iron(III) oxide by the thermolysis of iron(III) acetylacetonate in diphenyl ether. The effect of external factors on the morphology and size of resulting particles was studied. It was shown that increase in temperature and surfactant concentration in dispersion medium leads to considerable decrease of average particle size. This method is convenient, inexpensive, and low-toxic approach to the synthesis of nanosized iron(III) oxide with average particle size of 4–15 nm. It was found that the thermolysis of iron(III) acetylacetonate results in formation of nano-Fe_2O_3 of cubic structure. The ability of nano-Fe_2O_3 to reduction in hydrogen flow was studied by TPR. The reduction proceeds in three stages to give iron metal as a final product.

ACKNOWLEDGMENTS

This work was supported by the Russian Academy of Sciences (the program no. 25 of the Presidium of the RAS “Fundamental Chemical Aspects of Carbon Power Engineering,” the project “Research on the Design of Process for Oxidative Desulfurization of Oil and Petroleum Products in the Presence of Nanosized Oxide Catalytic Systems”).

REFERENCES

1. S. N. Khadzhiev, A. S. Lyadov, M. V. Krylova, and A. Y. Krylova, Petrol. Chem. **51**, 24 (2011).
2. S. Dadashi-Silab, Y. Yasemin, H. Acarb, and Y. Yagci, Polym. Chem. **6**, 1918 (2015).
3. D. B. Shieh, F. Y. Cheng, C. H. Su, et al., Biomater. **26**, 7183 (2005).
4. M. Mahmoudj, S. Sant, B. Wang, et al., Adv. Drug Deliv. Rev. **63**, 24 (2011).
5. B. Zhao, Y. Wang, H. Guo, et al., Mater. Sci. (Poland) **25**, 1143 (2007).
6. L. Zhang, W.-F. Dong, and H. -B. Sun, Nanoscale **5**, 7664 (2013).
7. H. Gu and M. D. Soucek, Chem. Mater. **19**, 1103 (2007).
8. X. Teng, X. Liang, S. Maksimuk, and H. Yang, Small **2**, 249 (2006).
9. H. S. Kil, Y. J. Jung, J. I. Moon, et al., J. Nanosci. Nano-technol. **15**, 6193 (2015).
10. M. Inouse, J. Phys.: Condens. Matter. **16**, 1291 (2004).
11. A. L. Willis, Z. Chen, J. He, et al., J. Nanomater. **2007**, 1 (2007).
12. W. C. Fernelius, Inorg. Synth. **2**, 27 (1946).
13. O. V. Sverdlova, *Electronic Spectra in Organic Chemistry* (Khimiya, Leningrad, 1985) [in Russian].
14. P. Scherrer and N. G. W. Gottingen, Math.-Phys. Kl. **2**, 96 (1918).
15. W. K. Jozwiak, E. Kaczmarek, T. P. Maniecki, et al., Appl. Catal. A: Gen. **326**, 17 (2007).

Translated by I. Kudryavtsev